A DSP-Based Resolver-To-Digital Converter for High Performance Electrical Drives Applications

Journal:	*Transactions on Industrial Electronics*
Manuscript ID:	15-TIE-1311
Manuscript Type:	Regular paper
Manuscript Subject:	Machines and Drives
Keywords:	AC motor drives, Position measurement, Control systems
Are any of authors IEEE Member?:	Yes
Are any of authors IES Member?:	No

COVER LETTER

Dear Associated Editor,

Dear Editorial Staff,

Hereafter we present a paper entitled:

"**A DSP-Based Resolver-To-Digital Converter for High Performance Electrical Drives Applications**"

In the last year many topic related papers have been submitted to IEEE Transaction on Industrial Electronics dealing with resolvers and Resolver to Digital Converters in particular.

The paper we are submitting presents a low cost, simple and highly accurate resolver-to-digital converter (RDC) for electrical drive applications. In order to validate the proposed system, the dynamic performance comparison between the RDC and a commercial optical encoder is analyzed and discussed. For this purpose, an experimental test bench is set up and accurately described. Both the simulation and experimental tests confirm the high reliability, stability and the good performances of the system. Moreover, the RDC is almost not affected by noise or external electromagnetic disturbances.

As a small amount of related papers focuses on high performance at low cost, we hope that our work may give a contribution to industrial development in the field of high-performance synchronous motor drives.

Best regards

The Authors

A DSP-Based Resolver-To-Digital Converter for High Performance Electrical Drives Applications

***Abstract*—This paper presents a low cost, simple and highly accurate resolver-to-digital converter (RDC) for electrical drive applications. In order to validate the proposed system, the dynamic performance comparison between the RDC and a commercial optical encoder is analyzed and discussed. For this purpose, an experimental test bench is set up and accurately described. Both the simulation and experimental tests confirm the high reliability, stability and the good performances of the system. Moreover, the RDC is almost not affected by noise or external electromagnetic disturbances.**

***Index Terms*—Electrical Drives, Speed, Position, Resolver, Tracking Loop.**

NOMENCLATURE

v_{sin},v_{cos}	resolver stator voltages
k	resolver stator-to-rotor transformation ratio
v_e	excitation voltage signal amplitude
ω_r	angular frequency of the excitation voltage
t	time variable
t_s	time instant corresponding to the signal sampling
θ	resolver shaft absolute angular position
ϕ	estimated resolver angular position
T	sampling period
K_P	proportional gain of the PI controller
K_I	integral gain of the PI controller
F_{PI}	transfer function of the PI controller in the z-domain
F_{ol}	open-loop transfer function in the z-domain
F_e	input/output position error transfer function in the z-domain
Θ	input position signal in the z-domain
Φ	output position signal in the z-domain
ζ	damping factor of the system
ω_n	characteristic frequency of the system
ω_0	IPMSM rated speed
a	acceleration constant
v	speed constant
f_{ref}	reference frequency of the input position signal
θ_{ref}	sinusoidal time-varying reference position signal
θ_x	amplitude of the sinusoidal reference position signal

I. INTRODUCTION

MANY SYNCHRONOUS electric motors require a very accurate position sensor compatible with a sinusoidal control. The purpose of such a control is to enable an efficient and smooth operation enhancing the comfort by limiting vibrations. In some cases related to mechanical constraints, we have to deal with through-shaft design [1]–[3]. One can quote, for example, power drives for Electric or Hybrid Electric Vehicles as well as for Electric Power Steering motor. More generally, these sensors need to keep a simple and robust design and a restricted number of parts as they are submitted to high vibration levels, a wide temperature range and speeds of several krpm.

Resolvers have been highly investigated in the technical literature [4], [5], especially from the signal conditioning and signal integration point of view in the whole control system [6]–[8]. In particular [9] have proposed low-cost method for converting the amplitudes of the sine/cosine transducer signals into a measure of the input angle without using look-up tables, also avoiding a poor precision in the comparison of the signals around their highly nonlinear peak regions, by using a simple technique that relies only on the alternating pseudo-linear segments of the signals. In [10] improves the software approach of transduction using the resolver-to-digital conversion, as the original approach takes sample at positive peak values of excitation signal which increases the system's complexity. Their paper applies an approach conceived to get information by taking sample at other positions in an excitation period.

The paper [11] focalizes instead on the typical faults of the sine-cosine resolvers and proposed a fault model based on the Mallat algorithm proposing then a processing circuit with a higher accuracy and reliability.

The paper [12] focalizes on a new technique to get the angular position with the help of an artificial neural network. As brushless drive performance may be conditioned by the high number of A/D converters and sensors with different bandwidth [13] propose a method for the reduction of such converter getting as a result a cheaper and reliable installation as confirmed by their experimental results on PSMS vector controlled drive.

The problems of self calibration and high accuracy in resolver to digital conversion (RDC) are the object of the papers [14] and [15] respectively. The second paper in particular considers an interesting combination of classical resolver and a second order decoupled double synchronous reference frame-based phase-locked loop (DSRF-PLL). Despite the apparent initial mathematical difficulty, Using the combined techniques and a standard DSP with a 12-bit analog-to-digital converter, a resolutions of up to 14 bits can be achieved with a small computation cost amounting about the 13% of the total (100 MIPs) [16].

[17] concentrate their investigations on the classical demodulation (or the one based on Chebishev Polynomials [18]) problem focusing on the integration technique starting from the zero crossing detection of the signals. The result of such investigation is the obtainment of actual envelopes of the signal waveforms by utilizing the phase relationship of the

integrated waveforms with the delayed carrier so that the noise and disturbance effects are averaged out and the achievable accuracy is improved without applying filters.

In this paper the Authors focus mainly on high accuracy rotor position estimation of electrical drives.

It is well known that industrial servo drive applications require a high accuracy estimation of the rotor position. This is particularly relevant in the fields of robotics and numerically controlled machine tools, in aerospace, satellite and military applications (i.e. in all those applications that involve transformations between rotational analog and digital information) in which little errors in rotor position estimation decay the servo drive position performance [19]–[21]. In these cases precise angle transducers, like absolute and incremental encoders or resolvers, are mechanically coupled to the shaft of the motors and quite often of the permanent magnet synchronous motors (PMSM). Resolvers, particularly, are angular speed and angle transducers well suited for applications requiring mechanical robustness and reliability over extremely long operational lifetimes [20]. Many advantages characterize these transducers such as: operation under severe atmospheric conditions, ability to work at high angular speed and acceleration, high accuracy, high noise immunity when used with integrated RDC, good immunity with respect to mechanical stresses and vibrations, possibility to transmit the output data over a long distance, and so on [19], [22]. The accuracy of the shaft angular speed and position measurement is fundamentally based on the assumption that ideal analog resolver signals are supplied to the RDC converter and on the high resolution of RDCs. Unfortunately high resolution RDCs are very expensive and many efforts were made in past works in order to simplify the converter topologies and to reduce its costs [23], [24].

An alternative solution for a RDC, based on a software approach, is proposed in this paper. The software can be implemented in a commercial digital signal processor (DSP) commonly used for servo drive control systems; the necessary hardware is limited to a few low-cost components that can be easily located on the power converter control board saving space on it. Main features of the software based RDC here presented are: high accuracy, simple set up, high reliability and stability and good performances. The experimental results by the comparison of the software based RDC output with that one of an precision encoder have shown that the accuracy of the digital speed and position measurement system is maintained and that this high accuracy can be reached reducing the costs, by using the alternative solution here proposed.

More in detail, this paper is structured as follows: Section II summarizes the problem statement. Section III describes the RDC software application with details about the control loop design. Section V presents both simulations and experimental results to demonstrate the effectiveness of the proposed solution. Finally Section VI summarizes conclusions.

II. Problem Statement

A resolver is a transducer commonly used in electrical drives in order to measure the absolute angular position (referred e.g. to the magnetic axis of one of its two stator windings) of the motor shaft. Thus, it is used to calculate the angular speed of the motor itself. The analog output sine and cosine modulated signals of the resolver are demodulated and, then, converted to a digital position signal and an analog speed signal by using a RDC. Basically, this converter is an integrated circuit (IC), which is usually mounted on the control board of the electric drive power converter [24].

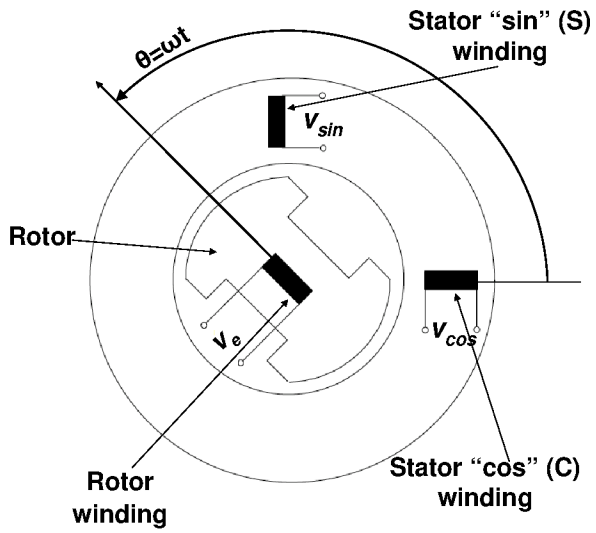

Figure 1. Simplified electrical scheme of the resolver.

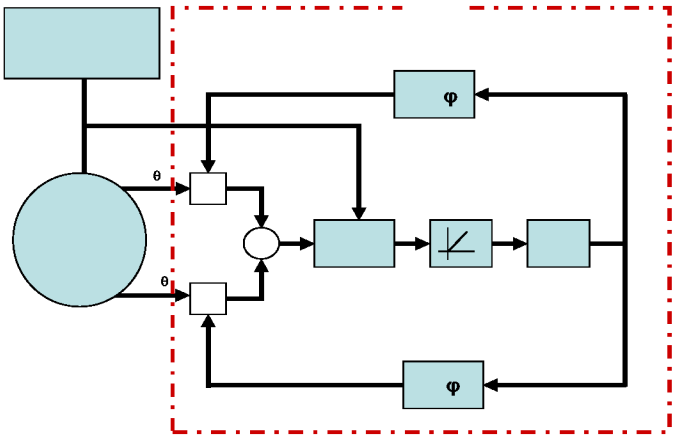

Figure 2. Schematic of a traditional resolver to digital converter.

The resolver is equipped with an excitation winding on its rotor, and with a two-phase winding on its stator and whose magnetic axes are 90° displaced each other [11], [25], [26]. A coupling transformer is used to supply (from an external power source) the resolver rotor winding with a sinusoidal excitation current. The simplified electrical scheme of a resolver is shown in Fig. 1. Its output consists of two sine wave voltage signals, whose amplitudes are modulated according to the sine and cosine of the shaft absolute position. The two signals are expressed in the time domain [24], [27]–[30] as follows:

$$\begin{cases} v_{\sin} = kv_e \left[\sin\theta \cos(\omega_r t) + \frac{1}{\omega_r}\frac{d\theta}{dt}\cos\theta \sin(\omega_r t) \right] \\ v_{\cos} = kv_e \left[\cos\theta \cos(\omega_r t) + \frac{1}{\omega_r}\frac{d\theta}{dt}\sin\theta \sin(\omega_r t) \right] \end{cases} \quad (1)$$

If ω_r is high enough with respect to the maximum rotor angular speed $d\theta/dt$ (in our case for $\omega_r = 2 \cdot \pi \cdot f = 2 \cdot \pi \cdot 5000 = 31415$ rad/s and $\frac{d\theta}{dt}\big|_{max} = 400$ rad/s), the second term of sum in expressions (1) can be neglected, leading to the following approximated equation:

$$\begin{cases} v_{\sin} = kv_e \left[\sin\theta \cos\left(\omega_r t\right)\right] \\ v_{\cos} = kv_e \left[\cos\theta \cos\left(\omega_r t\right)\right] \end{cases} \quad (2)$$

Each of the signals of (2) must be conditioned through a differential amplifier in order to refer them to a common ground. This allows to amplify the signals and to reject possible existing common mode noise components. Both signals are, then, sent to the analog inputs of the R/D converter, which demodulate and processes them giving the angular position of the shaft as a digital output and its angular speed as an analog out. Figure 2 shows the simplified block diagram of the traditional position estimation system using the integrated RDC. In order to summarize the traditional R/D conversion, it is assumed that the current position output is ϕ (see Fig. 2). The input signals v_{sin} and v_{cos} are multiplied by $\cos\phi$ and $\sin\phi$, respectively, and then subtracted and demodulated. Thus, the result is proportional to $\sin\Delta\theta = \sin(\theta - \phi)$ (i.e. to the sine of the position error). Finally, this error is delivered to the integrator, which allows to obtaining the speed analog signal, and the VCO (Voltage Controlled Oscillator) for the digital position estimation ϕ [24], [27], [31].

The traditional solution previously described results expensive due to the cost of the integrated RDC, which is almost equal to the cost of the resolver. Furthermore, the dynamic and static performances of such RDC ICs are fixed or can be set up by using additional passive components, such as resistors and capacitors. As a consequence, both stability and performance of the position tracking loop depend on the stability of these components.

On the contrary, the proposed high accuracy software-based RDC presents many advantages in terms of noise immunity, reliability, stability and simplicity. Another great advantage is the reduced cost of the RDC, due to the suppression of the additional discrete components, of the complex electronic circuit layout in traditional RDCs. In addition, the implementation on DSPs is very simple, avoiding the need of additional hardware on the converter's control board. Moreover, the flexibility of the entire system is improved thanks to the tuning of all that parameters on which both the static and dynamic performances of the position tracking loop depend. Finally, a significant increase in resolution can be achieved for the position estimation using the over sampling technique and avoiding the use of high performance analog to digital converters (ADC) [19], [32].

III. Description of the Software Based Resolver to Digital Converter

In this section, the software RDC system and its operation are presented and extensively described. In addition, several test results are hereafter reported and discussed.

A. Analog Signal Conditioning Network

The electronic analogue interface scheme and the block diagram of the proposed software based RDC are shown in Fig. 3 and Fig. 4, respectively. The 5 kHz sinusoidal excitation (carrier) signal for the resolver is generated by the dSPACE® board through a PWM generator operating at 40 kHz. The carrier signal is then sent to an electronic conditioning network which is composed by a 2^{nd} order analogue band-pass filter (BPF). The BPF is centered at 5 kHz with a bandwidth of 2.5 kHz being able to filter the higher harmonics of the signal generated by the dSPACE® board. In addition, a power amplifier is used to amplify the sinusoidal signal and to supply the rotor excitation winding.

The sine and cosine output signals are delivered to a differential amplifier and passed through an anti-aliasing RC filter. Finally, the signals are fed to the two 12 bit analog to digital converters (ADC) of the dSPACE® board (see Appendix for characteristics).

B. Closed Loop Position Tracking System

The simplified block diagram of the closed loop position tracking implemented on the dSPACE® control board, is shown in Fig. 4. This algorithm is based on the oversampling technique. As a matter of fact, the sine and cosine modulated resolver outputs are sampled at 8-times the excitation signal frequency (i.e. 8*5 kHz=40 kHz). The ADC sampling is also synchronized to the DAC which generates the sinusoidal excitation signal for the resolver, by using the same interrupt of the dSPACE® board (see Fig. 4). Each of the digitized sine and cosine modulated signals are then filtered through a digital 16th order FIR band-pass filter, reducing the signal bandwidth to 5000±1250 Hz. Afterwards, the downsampling technique is used reducing the sampling rate to 5 kHz, which is achieved by selecting only one sample from a group of consecutive 8 samples of the sine - cosine signals. This technique allows to demodulate the signals, enabling the sine and cosine for the position and speed closed loop tracking system [24]. With this decimation, the resolution has been improved of 1.5 bits [32], [33]. Figure 5 shows an example of the two digitally demodulated sine and cosine signals at 4000 rpm.

In particular, with the previously mentioned synchronization and decimation, the output signals of the resolver are always sampled at the same instant within a period of the carrier signal, i.e. at:

$$t_s = t_0 + \frac{2\pi}{\omega_r} n \quad (3)$$

where *n* is an integer number.

Thus, by taking (3) into account, (2) can then be rewritten as:

$$\begin{cases} v_{\sin} = kv_e \left[\sin\theta \cos\left(\omega_r t_s\right)\right] = \\ v_{\cos} = kv_e \left[\cos\theta \cos\left(\omega_r t_s\right)\right] = \end{cases} \begin{cases} = kv_e \left[\sin\theta \cos\left(\omega_r t_0\right)\right] = k' \sin\theta \\ = kv_e \left[\cos\theta \cos\left(\omega_r t_0\right)\right] = k' \cos\theta \end{cases} \quad (4)$$

with $kv_e \cos\left(\omega_r t_0\right) = k' = const.$

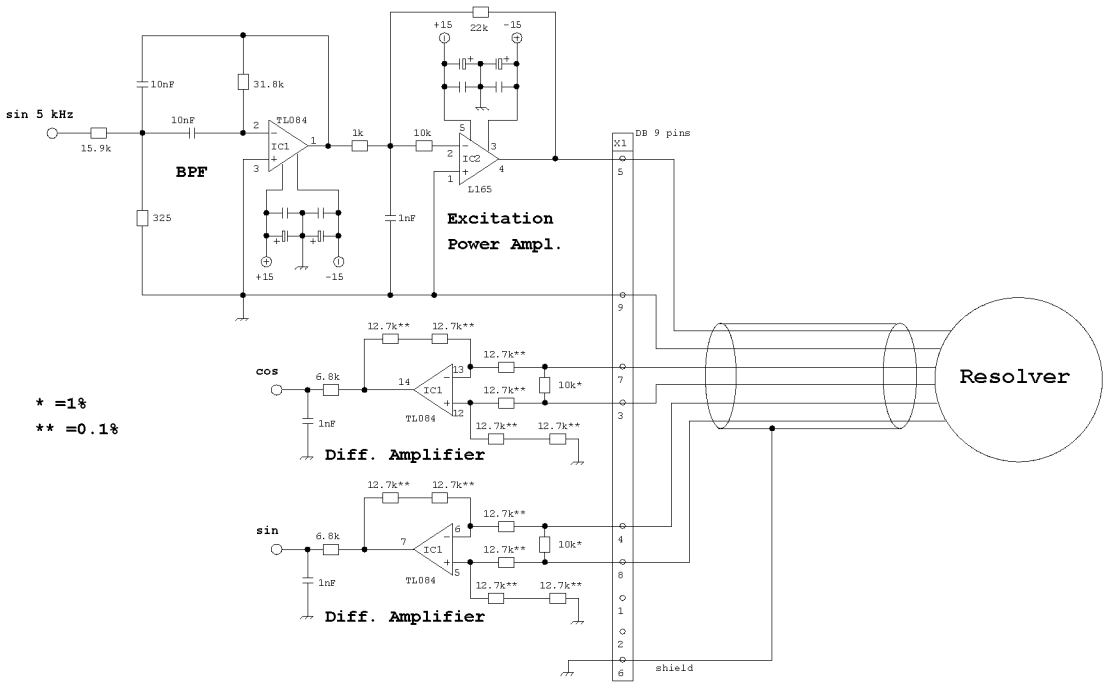

Figure 3. The resolver analog interface.

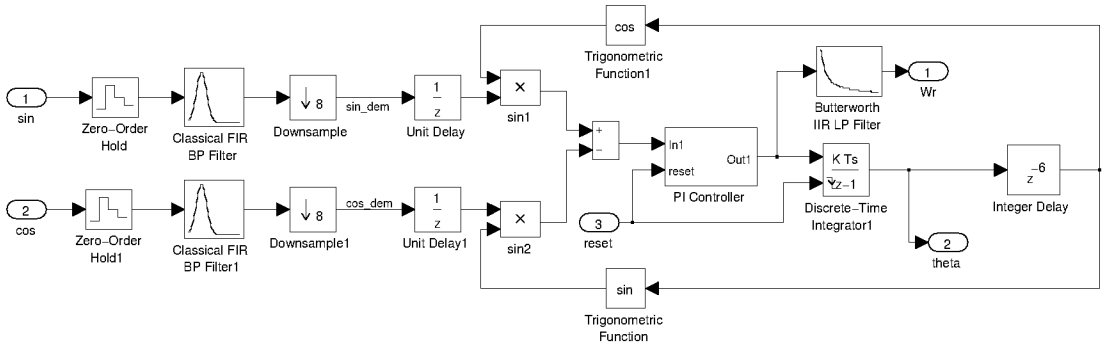

Figure 4. Simplified block scheme of the software based RDC.

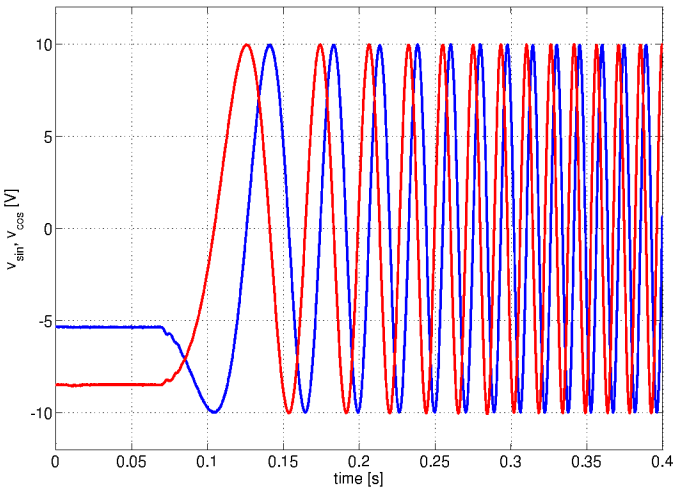

Figure 5. The demodulated sine and cosine signals during an acceleration from 0 to 4000 rpm.

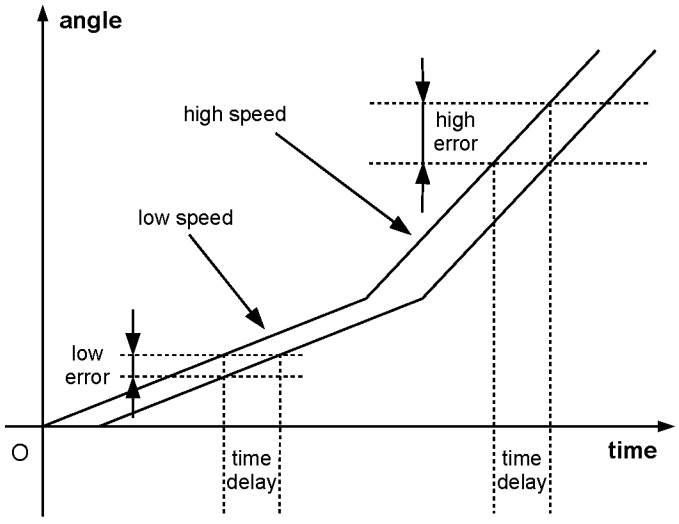

Figure 6. Combined effect of the FIR filter delay and the angular speed on the angle error.

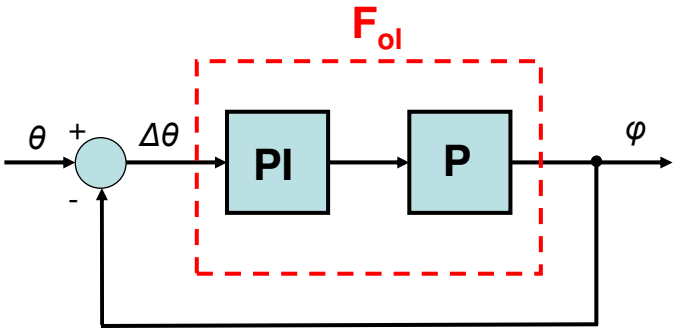

Figure 7. Simplified block diagram of the closed loop position tracking system.

The demodulated sine and cosine signals v_{sin} and v_{cos} are multiplied by cosϕ and sinϕ, respectively, and, then, subtracted each other. The obtained output signal is proportional to the sine of the error between the resolver shaft angle θ and the estimated angle ϕ, as shown by the following equation:

$$v_{err} = k' \left(\sin\theta\cos\phi - \cos\theta\sin\phi\right) = k'\sin\left(\theta - \phi\right) \quad (5)$$

The error signal v_{err} is then processed by the PI controller, in order to minimize it, obtaining the speed signal. The final operation, which closes the control loop, consists into the integration of the PI output signal, in order to make the estimated angle ϕ available at the output of the RDC.

The time delay introduced by the FIR BPF determines an error of the estimated angle ϕ with respect to θ. This error, which is proportional to the resolver angular speed, can be graphically explained in Fig. 6. A compensation of this error is possible in steady state operation (i.e at constant speed), by delaying the angle ϕ signal by a specified amount of samples. This fact will be extensively discussed and experimentally demonstrated in section V.

C. Set-up of the Position Tracking Loop Parameters

When the position error $\Delta\theta = \theta - \phi$ is small enough, then $\sin\left(\Delta\theta\right) \cong \Delta\theta$ and the block diagram of the position tracking loop represented in Fig. 4 can be redrawn in a more simple manner, as shown in Fig. 7.

By considering the forward Euler integration method, it is possible to carry out the equations that characterize the RDC conversion procedure. With reference to Fig. 7 the transfer function referred to the process P is given by, :

$$P(z) = k'\frac{T}{z-1} \quad (6)$$

The proportional and the integral gain of the PI controller are expressed by:

$$F_{PI}(z) = \frac{K_P(z-1) + K_I T}{z-1} \quad (7)$$

The open loop transfer function of the proposed closed loop control system is expressed in the z-domain as:

$$F_{ol}(z) = k'T \cdot \frac{K_P(z-1) + K_I T}{(z-1)^2} \quad (8)$$

and the input/output error transfer function is given by:

$$F_e(z) = \frac{\Theta - \Phi}{\Theta} = \frac{(z-1)^2}{(z-1)^2 + k'TK_P(z-1) + k'K_I T^2} \quad (9)$$

If the input signal is a parabolic ramp, i.e. during acceleration, the steady-state error is:

$$e = \lim_{z\to 1} F_e(z) \cdot \frac{aT^2}{(z-1)^2} = \lim_{z\to 1} \frac{aT^2}{(z-1)^2 + k'TK_P(z-1) + k'T^2K_I} = \frac{a}{k'K_I} \quad (10)$$

if K_I is high enough with respect to a, then the related error can be minimized. Therefore, for a fixed error the maximum acceleration can be calculated by 10. For example, if the position error $e*$ during a constant acceleration has to be kept within 1 degree, the maximum acceleration will be:

$$a_{max} = e^* \cdot k' \cdot K_I = \frac{\pi}{180} \cdot 1 \cdot k' \cdot K_I = 261\,[rad/s^2] \quad (11)$$

If the input signal is a linear ramp, i.e. when the speed assumes a constant value, the position error is:

$$e = \lim_{z\to 1} F_e(z) \cdot \frac{\omega T}{z-1} = \lim_{z\to 1} \frac{\omega T(z-1)}{(z-1)^2 + k'TK_P(z-1) + k'T^2K_I} = 0 \quad (12)$$

Thus, this error is theoretically null. However, the experimental tests of section V will demonstrate that this error is not null.

The closed-loop RDC transfer function related to the simplified block of Fig. 7 is given by:

$$F_{cl}(z) = \frac{\Phi}{\Theta} = \frac{TK_P(z-1) + K_I T^2}{(z-1)^2 + k'K_P T(z-1) + k'K_I T^2} \quad (13)$$

By assuming two complex conjugate dominant poles, the following PI parameters approximated set-up results:

$$K_P = \frac{2\zeta\omega_n}{k'} \quad (14)$$

$$K_I = \frac{\omega_n^2}{k'} \quad (15)$$

Therefore, by selecting the most satisfactory values for both the natural frequency and the damping factor, the RDC can be set in a very easy and quick way.

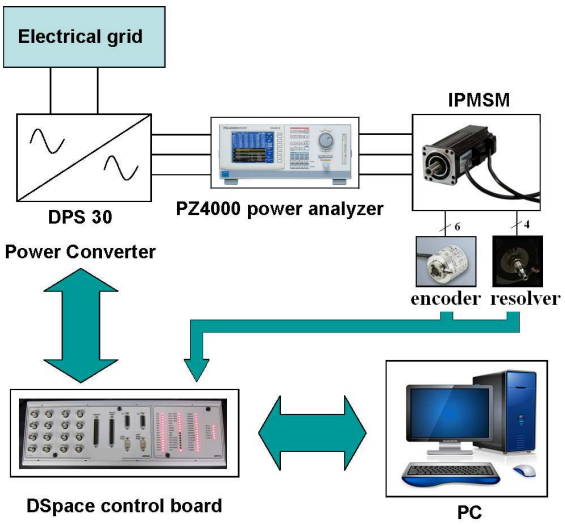

Figure 8. Schematic representation of the test bench.

IV. IPMSM and RDC Test Bench

An experimental test bench has been set up at the SDES Laboratory of the DEIM (Department of Energy, Information engineering and Mathematical models, University of Palermo, Italy) and a schematic representation of the proposed test bench is shown in Fig. 8.

The IPMSM under test is driven by a three-phase VSI (Automotion Inc., type DPS 30-A) and it is connected to a hysteresis brake (Magtrol Inc., type DSP6001), in order to perform experimental tests at different load conditions. A three-phase power analyzer (Yokogawa Inc., type PZ 4000) is used to measure the phase voltages, currents and the electrical power. In order to measure the motor speed, a two poles ARTUS resolver (type 26SM19 RX452 CO1F/00) and an optical incremental encoder (LTN Servotechnik, 1024 ppr, type G36 W) are connected to the IPMSM shaft, as shown in Fig. 9 and Fig. 10, respectively.

The DPS 30 is connected to a dSPACE® rapid prototyping control board to drive the IGBT bridge. Furthermore, two current sensors are integrated onto the electronic power converter module and their output signals are sent to the dSPACE® board. The output signals of the PWM generator are directly fed by the dSPACE® board to the IGBT driver. The real-time control of the main drive electrical and mechanical quantities and its supervision are performed by the dSPACE®-based electrical drive user interface, which is shown in Fig. 11. The PI parameters have been chosen to reach a 250 Hz closed loop bandwidth (see Appendix).

Figure 13 shows a simplified block diagram of the proposed RDC, while the RDC test bench during the related measurements is shown in Fig. 12.

V. Simulations, Experimental Tests and Results

In this section several simulation and experimental tests for the validation of the proposed system are summarized and discussed. These tests were performed in order to experimentally determine the frequency response of the RDC and

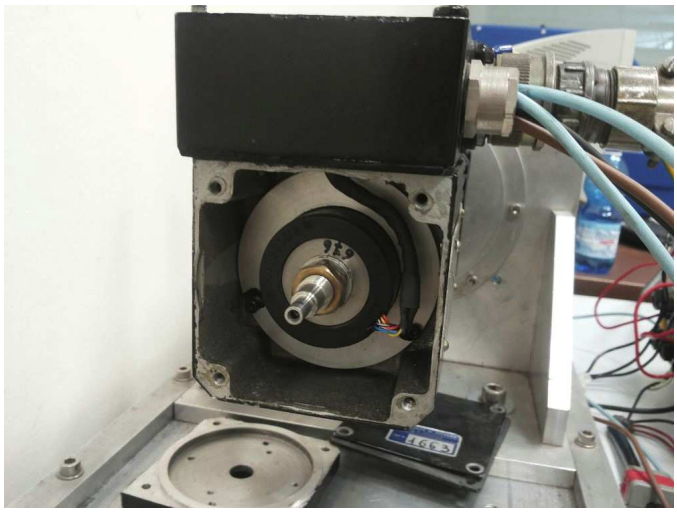

Figure 9. Artus resolver used during the experimental tests.

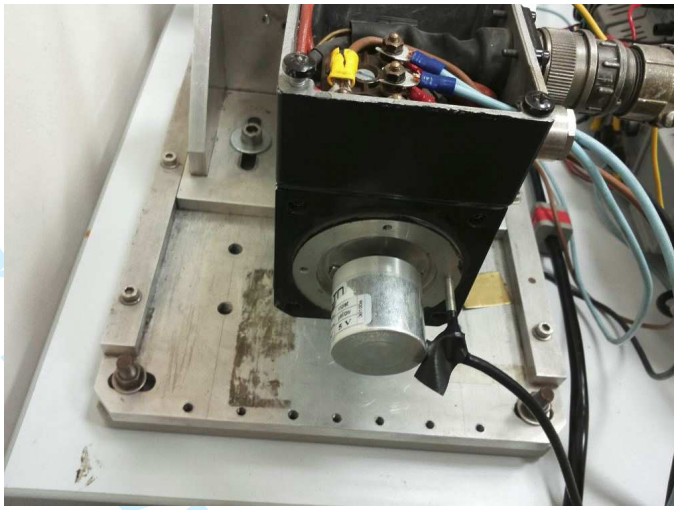

Figure 10. Optical encoder used during the experimental tests.

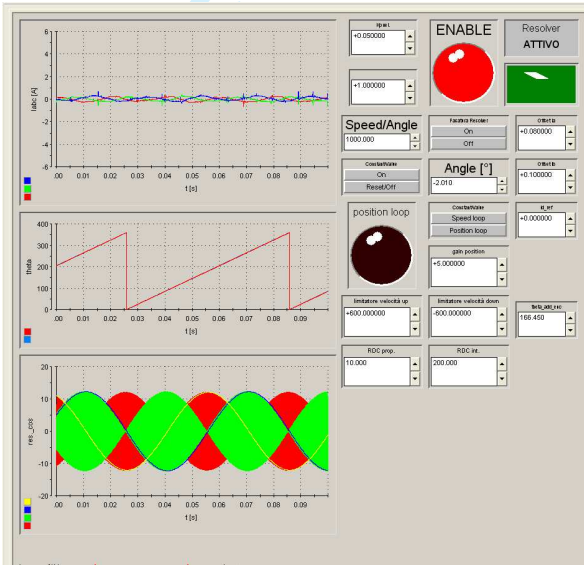

Figure 11. dSPACE® user interface.

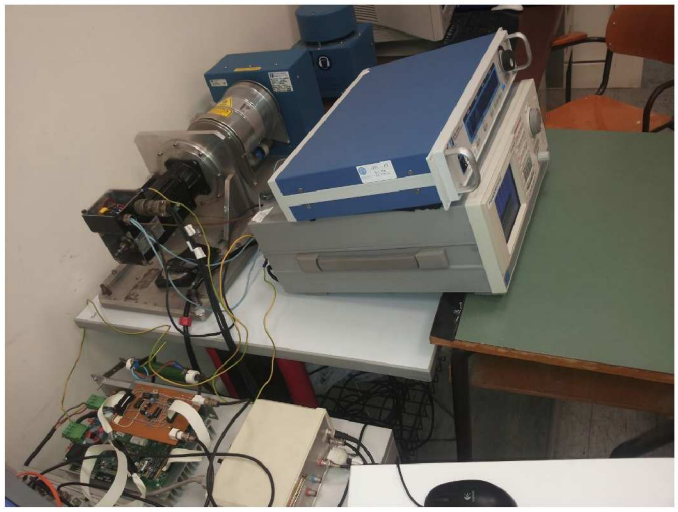

Figure 12. The RDC test bench.

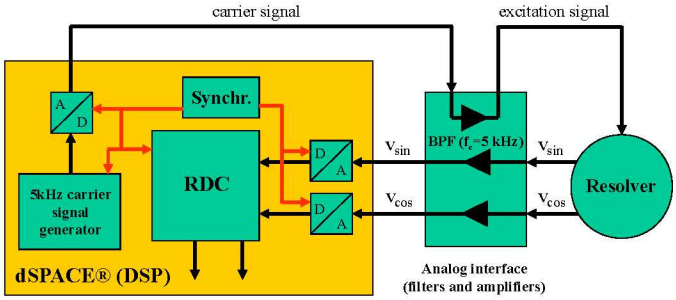

Figure 13. The RDC simplified block diagram.

compare it with the response obtained from the approximated mathematical model.

For this purpose a sinusoidal time-varying reference position signal was fixed, according to the following equation:

$$\theta_{ref}(t) = \theta_x \sin(2\pi f_{ref} t) \tag{16}$$

where θ_x has been set to 10°, while f_{ref} has been varied from 0.01 Hz to 1000 Hz. In addition, the proportional and integral PI gains were set to 10 and 1500, respectively. The output position signal will be approximatively given by :

$$\phi_{out} \cong \phi_x sin(2\pi f_{ref} t + \rho) \tag{17}$$

where ρ is the phase-shift between the output and the input signals. The ϕ_x/θ_x ratios and ρ have been computed for several frequency values and have been used in order to draw the frequency response of the non linear RDC closed-loop system.

However, due to the non linearity of the proposed system, a relevant steady-state position error has occurred during the experimental tests, produced by the closed-loop RDC (see Fig. 6). This error is strictly dependent on ω_n and on the number of delayed samples. In order to determine the relationship between the position error speed of the input signal and the delay, several tests have been carried out by varying the output delay from z^0 to z^{-7} at different percentages of the IPMSM rated speed. With evidence of Fig. 14, which shows the average

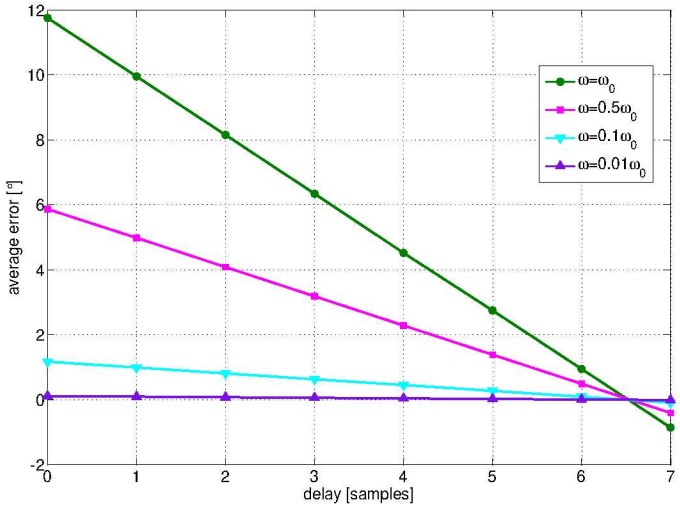

Figure 14. Average position error as function of the number of delayed samples.

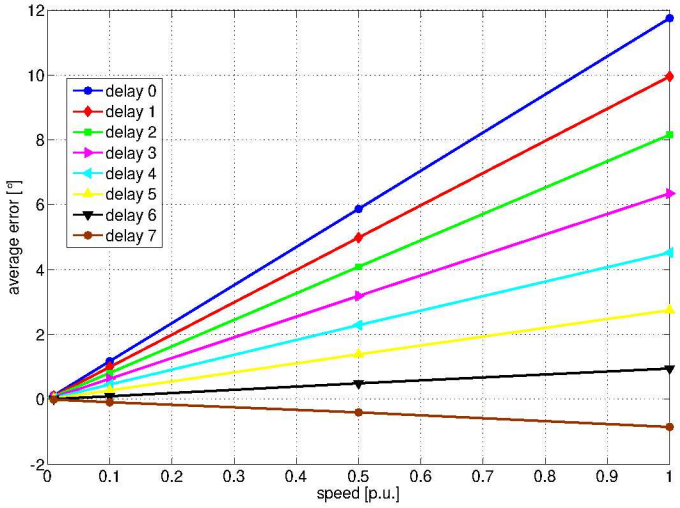

Figure 15. Average position error as function of the IPMSM speed.

position error/delayed sample trend at 1%, 10%, 50% and 100% of ω_0, by increasing the number of delayed samples the position error decreases almost with a linear trend. However, for a z^{-7} integer delay the error turns into negative values. These data can be also analyzed from the graph of Fig. 15, which shows the error as function of the IPMSM speed and parametrized for the number of delayed samples. Thus, from the reported results, a six-step delay block has been introduced into the RDC system, as shown in Fig. 4 and, therefore, the position error has been minimized.

The introduction of the six-step delay has not affected the set-up equations described in section III-C. As a matter of fact, by comparing the frequency response experimentally determined with the frequency response computed from the RDC approximated mathematical model (see Fig. 16a), it can be noticed that the two frequency responses have an almost similar shape. Moreover, the phase response has been compared with the approximated one, as shown in Fig. 16b. From the plotted characteristics it is evident that the two trends

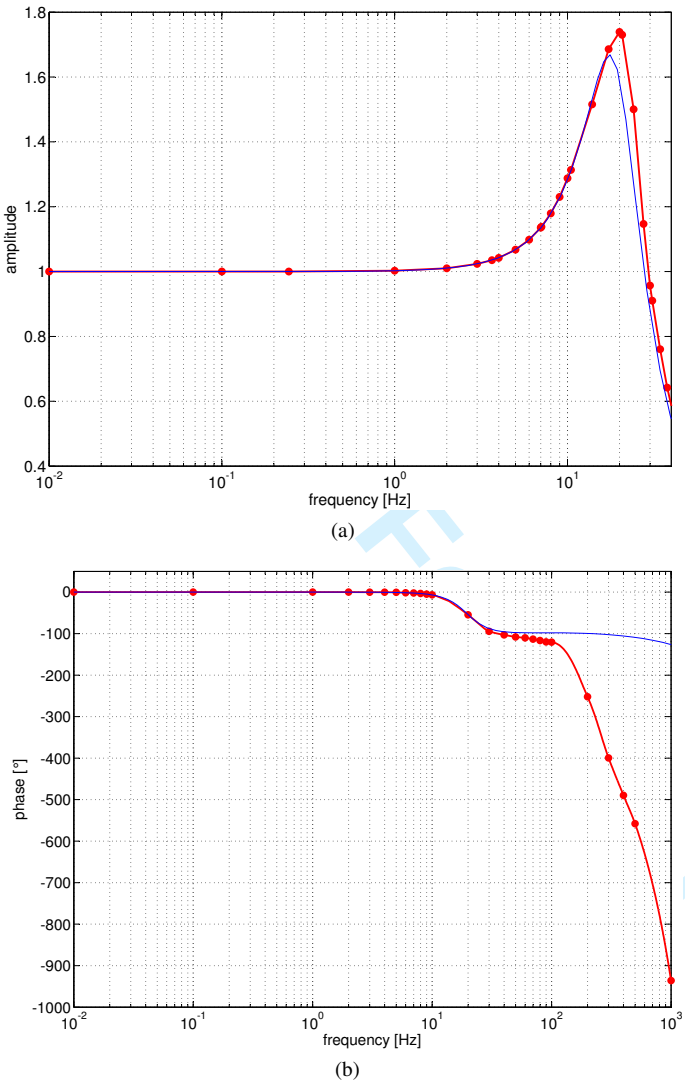

Figure 16. Frequency response comparison between the RDC (red) and the mathematical model (blue): (a) amplitude and (b) phase.

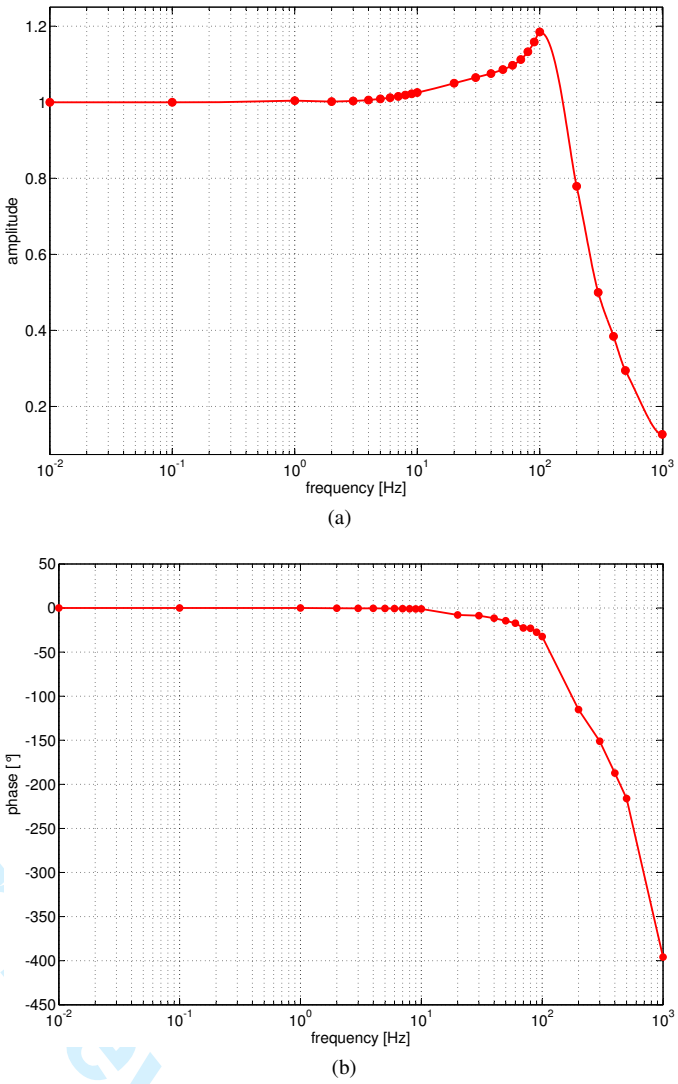

Figure 17. Frequency response phase comparison between the RDC (red) and the mathematical model (blue) at 90°: (a) amplitude and (b).

are very close to each other, except for the gap detected in the frequency range from 20 Hz to 200 Hz, with a maximum phase difference gap of about 90° at 120 Hz, which is assumed to be not relevant for the RDC tracking efficiency.

The reliability of the proposed model is confirmed also for high values of the reference position signal amplitude. In fact, by setting the amplitude at 90° and by varying the input position reference frequency from 0.01 Hz to 1000 Hz, the computed input/output response and the phase response have been plotted. From the obtained results, shown in Fig. 17a and 17b, it can be noticed that the resonant peak is shifted towards higher frequencies and its value has been decreased, which is due to the non linear behavior of the RDC closed-loop system. Thus, for high variations of the input signal, an improvement of the signal fidelity is achieved.

In addition, the root locus corresponding to the approximated model above reported is shown in Fig. 18, which clearly demonstrates that there is a good margin for the RDC open-loop gain increase, if a higher tracking speed is needed. Therefore, the proposed simplified model has been successfully validated as for (14) and (15), even with the introduction of the six-step delay.

Moreover, a dynamic performance comparison between the RDC and the commercial optical encoder described in sec. IV has been developed. In particular, Fig. 19a and Fig. 19b show the trends of the position signals acquired with the resolver (and the proposed software based resolver to digital converter) and with the 1024 point per revolution (ppr) optical encoder, respectively, whereas Fig. 20 shows the error between the two signals as function of time. These measurements were carried out during an acceleration test of the motor from 0 to 4000 rpm. In addition, the angular speed measured from both encoder and resolver has been acquired and plotted in Fig. 21. From the details reported in the same figure, it can be noticed that the two trends are coincident, except for the fact that the encoder output signal is affected by disturbances.

Almost the same results in terms of dynamic performances and resolution can be noticed during a deceleration test from 4000 rpm to 0 rpm. The recorded angular speed signals measured from the RDC and encoder during the above men-

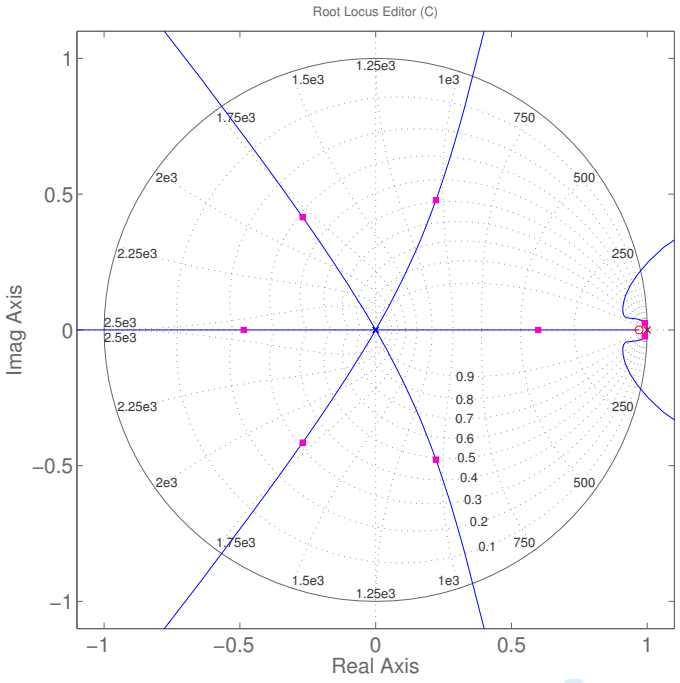

Figure 18. Root locus of the proposed model.

tioned test are reported in Fig. 22. As mentioned before, the difference between the two recorded signals isn't appreciable. Therefore, the excellent tracking performance of the software based RDC is demonstrated.

The accuracy of the proposed RDC can be appreciated more specifically for relatively low speeds. For this purpose, the motor has been driven with a reference speed of 10 rpm and the speed output signals coming from both resolver and encoder have been plotted in Fig. 23. This figure demonstrates that the performance of the RDC is the same both at low and at high speed, while the encoder is affected by disturbances due mainly to quantization, which leads to a change on its resolution.

Other interesting results are reported in Fig. 24, which shows the angular speed detected from the RDC at 0 rpm, when the motor is disconnected from its power supply. In addition, the related RDC position output signal is depicted in Fig. 25. As for the previous low speed test, it can be noticed that the angular speed signal obtained from the RDC seems to be quite free from noise.

VI. Conclusions

This paper has presented a low cost software-based RDC. The simulation and experimental results have confirmed the high accuracy of the signal acquisition of both the position and the angular speed of the resolver shaft. In addition, it has been demonstrated that the implementation of the RDC in a digital PMSM drive is very simple (only one DAC, two ADC and a commercially available DSP are needed), as well as the position tracking loop algorithm. The software approach in this algorithm ensures no parameter variations (caused by temperature variations or component drifts) and the output

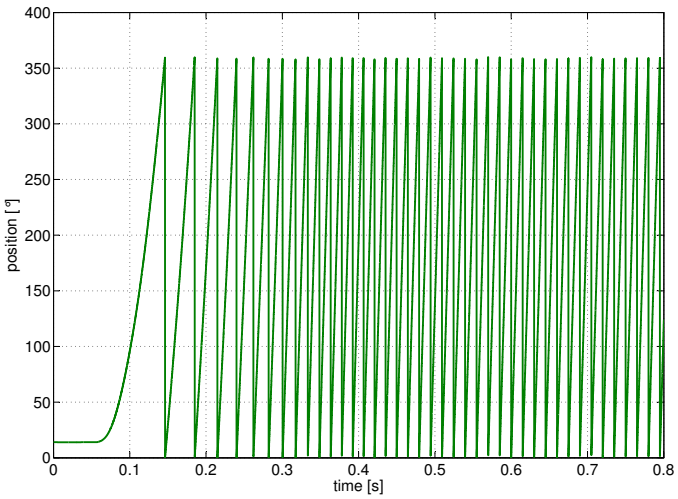

(a)

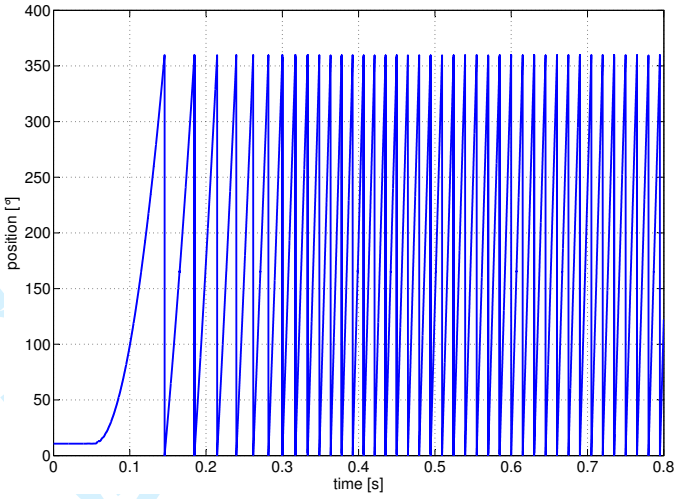

(b)

Figure 19. Resolver (a) and encoder (b) position signals during the acceleration test from 0 to 4000 rpm.

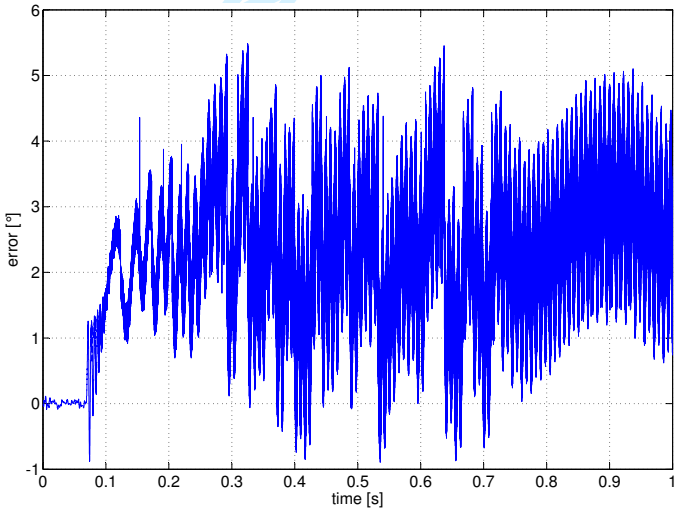

Figure 20. Error between resolver and encoder position signals during the acceleration test from 0 to 4000 rpm.

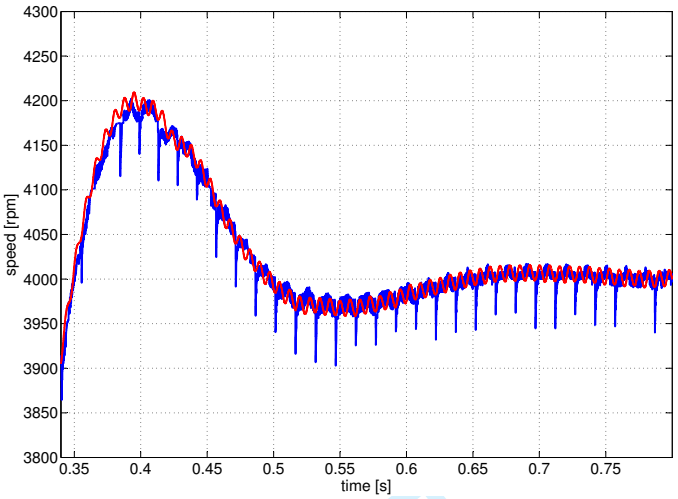

Figure 21. Angular speed signals detected from the resolver (red) and encoder (blue) during the acceleration test from 0 to 4000 rpm.

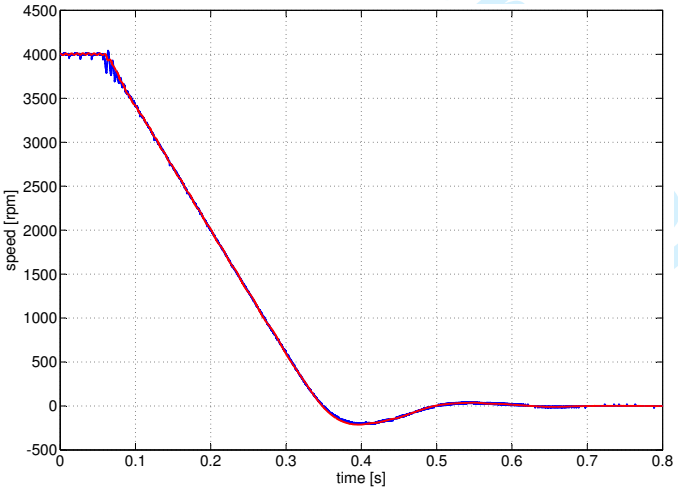

Figure 22. Comparison between the speed detected from the RDC (red) and the optical encoder (blue) during a brake operation from 4000 to 0 rpm.

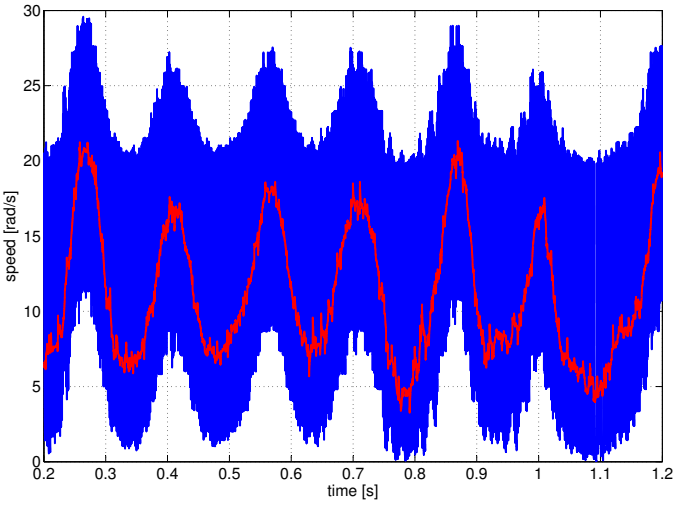

Figure 23. Comparison between the angular speed detected from the RDC (red) and the optical encoder (blue) with ω_{ref}=10 rpm.

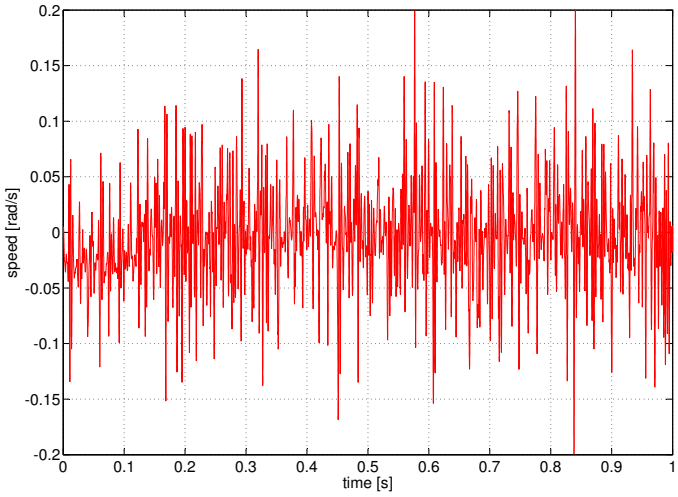

Figure 24. RDC speed output signals at 0 rpm.

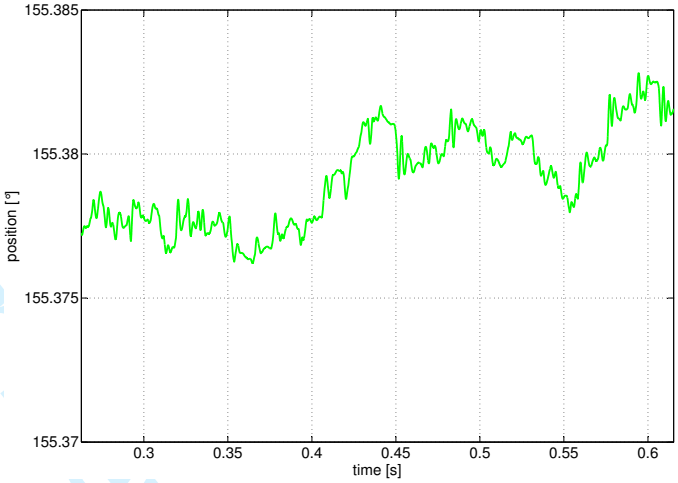

Figure 25. RDC output position signals at 0 rpm.

signals are almost not affected by noise or external electromagnetic disturbances. Moreover, the comparison between the RDC and a commercial encoder output signals have shown the high stability and good performances of the proposed system.

APPENDIX

The parameters of the PI controller were chosen in order to achieve a damping factor ζ = 0.614 and a characteristic frequency ω_n= 122 rad/s.

The ADCs of the dSPACE® board have a resolution of 12 bit, conversion time of $0.8 \cdot 10^{-6}$ s and an input voltage range of $\pm$10 V. The DACs, instead, have a resolution of 14 bit, conversion time of $6 \cdot 10^{-6}$ s, an output voltage range of $\pm$10 V and a maximum output current of $\pm$5 mA.

The transformation ratio of the ARTUS resolver is 0.5.

REFERENCES

[1] S.-I. Park and K.-C. Kim, "Study on the optimal design of a novel slotless resolver by fem," *Magnetics, IEEE Transactions on*, vol. 50, pp. 1–4, Nov 2014.

[2] X. Ge, Z. Zhu, R. Ren, and J. Chen, "A novel variable reluctance resolver with nonoverlapping tooth 2013;coil windings," *Energy Conversion, IEEE Transactions on*, vol. 30, pp. 784–794, June 2015.

[3] C.-S. Jin, I.-S. Jang, J.-N. Bae, J. Lee, and W.-H. Kim, "Proposal of improved winding method for vr resolver," *Magnetics, IEEE Transactions on*, vol. 51, pp. 1–4, March 2015.

[4] C. Sivappagari and N. Konduru, "Review of rdc soft computing techniques for accurate measurement of resolver rotor angle," *Sensors and Transducers*, vol. 150, no. 3, pp. 1–11, 2013.

[5] C. Sivappagari and N. Konduru, "High accuracy resolver to digital converter based on modified angle tracking observer method," *Sensors and Transducers*, vol. 144, no. 9, pp. 101–112, 2012.

[6] N. Abou Qamar, C. Hatziadoniu, and H. Wang, "Speed error mitigation for a dsp-based resolver-to-digital converter using autotuning filters," *Industrial Electronics, IEEE Transactions on*, vol. 62, pp. 1134–1139, Feb 2015.

[7] C.-C. Hou, Y.-H. Chiang, and C.-P. Lo, "Dsp-based resolver-to-digital conversion system designed in time domain," *Power Electronics, IET*, vol. 7, pp. 2227–2232, September 2014.

[8] Y. Wang, Z. Zhu, and Z. Zuo, "A novel design method for resolver-to-digital conversion," *Industrial Electronics, IEEE Transactions on*, vol. 62, pp. 3724–3731, June 2015.

[9] L. Ben-Brahim, M. Benammar, and M. Alhamadi, "A resolver angle estimator based on its excitation signal," *IEEE Trans. on Ind. Electron.*, vol. 56, pp. 574–580, February 2009.

[10] Y. Zu and W. Yan-Ming, "An approach based on ad converted resolver demodulation," in *20IO 3rd International Conference on Advanced Computer Theory and Engineering(ICACTE)*, vol. 5, pp. 192–195, IEEE, 2010.

[11] Q.-X. Zhou, "Research on the signal process circuit and fault diagnosis of sine-cosine resolver," in *Electric Information and Control Engineering (ICEICE), 2011 International Conference on*, pp. 5281–5284, April 2011.

[12] C. Raymundo, W. Suemitsu, and J. Pinto, "Robust measurement of angular position using resolver sensor and adaline neural networks," in *11th Brazilian Power Electronics Conference, COBEP 2011* (IEEE, ed.), IEEE, 2011.

[13] R. Cordero, W. Suemitsu, J. Pinto, A. Soares, and R. Capitanio, "Application of frequency domain multiplexing for the reduction of adcs in vector control of pmsm," in *38th Annual Conference on IEEE Industrial Electronics Society, IECON 2012*, pp. 1690–1695, 2012.

[14] J. Faber, "Self-calibration and noise reduction of resolver sensor in servo drive application," in *9th International Conference on ELEKTRO 2012*, 2012.

[15] J. Bergas-Jane, C. Ferrater-Simon, G. Gross, R. Ramirez-Pisco, S. Galceran-Arellano, and J. Rull-Duran, "High-accuracy all-digital resolver-to-digital conversion," *IEEE Trans. on Ind. Electron.*, vol. 59, pp. 326–333, January 2012.

[16] X. Shi and B. Wei, "An open-loop digital solver of shaft angle based on dsp," in *WIT Transactions on Information and Communication Technologies*, vol. 51, pp. 105–111, 2014.

[17] N. Lin Htun Aung, C. Bi, A. Al Mammun, C. Su Soh, and Y. YinQuan, "A demodulation technique for spindle rotor position detection with resolver," *IEEE Trans. on Magn.*, vol. 49, pp. 2614–2619, June 2013.

[18] H. Yang, Y. Zhao, C. Ye, and Z.-L. Wang, "Rapid resolver angle demodulation algorithm based on chebyshev polynomial," *Zhongguo Guanxing Jishu Xuebao/Journal of Chinese Inertial Technology*, vol. 21, no. 4, pp. 530–535, 2013.

[19] M. Staebler, "TMS320F240 DSP Solution for Obtaining Resolver Angular Position and Speed ," Texas Instruments, Application Report, February 2000.

[20] C. Lee, R. Hill, and K. Nies, "Total ionizing dose radiation characterization of the natel hsrd1056rh resolver-to-digital converter hybrid," in *Radiation Effects Data Workshop, 1992. Workshop Record., 1992 IEEE*, pp. 48–52, 1992.

[21] W. He, X. Xu, and Z. Shi, "Error analysis of a novel resolver-to-digital converter," *Advanced Materials Research*, vol. 542-543, pp. 695–698, 2012.

[22] B. Murray and W. Li, "A digital tracking r/d converter with hardware error calculation using a tms320c14," in *Power Electronics and Applications, 1993., Fifth European Conference on*, pp. 472–477 vol.4, Sep 1993.

[23] C.-H. Yim, I.-J. Ha, and M.-S. Ko, "A resolver-to-digital conversion method for fast tracking," *Industrial Electronics, IEEE Transactions on*, vol. 39, pp. 369–378, Oct 1992.

[24] C. Attaianese, G. Tomasso, and D. De Bonis, "A low cost resolver-to-digital converter," in *Electric Machines and Drives Conference, 2001. IEMDC 2001. IEEE International*, pp. 917–921, 2001.

[25] C. Sivappagari and N. Konduru, "Modified ato algorithm based high accuracy rdc using pulse excitation," in *1st International Conference on Automation, Control, Energy and Systems, ACES 2014*, 2014.

[26] W. Xu, J. G. Zhu, Y. Zhang, Z. Li, Y. Li, Y. Wang, Y. Guo, and Y. Li, "Equivalent circuits for single-sided linear induction motors," *Industry Applications, IEEE Transactions on*, vol. 46, pp. 2410–2423, Nov 2010.

[27] D. Hanselman, "Resolver signal requirements for high accuracy resolver-to-digital conversion," in *Industrial Electronics Society, 1989. IECON '89., 15th Annual Conference of IEEE*, pp. 486–493 vol.2, Nov 1989.

[28] A. Di Tommaso and R. Miceli, "A new high accuracy software based resolver-to-digital converter," in *Industrial Electronics Society, 2003. IECON '03. The 29th Annual Conference of the IEEE*, vol. 3, pp. 2435–2440 Vol.3, Nov 2003.

[29] Q. Zhou, Y. Zhang, Y. Zhou, and D. Yu, "Error analysis and compensation method research of airborne reluctance rvdts," *Lecture Notes in Electrical Engineering*, vol. 296 LNEE, no. VOL. 1, pp. 199–207, 2014.

[30] C. Sivappagari and N. Konduru, "High tracking accuracy of software based rdc using various excitation signals," in *2014 International Conference on Advances in Electrical Engineering, ICAEE*, 2014.

[31] R. Stewart and E. Pfann, "Oversampling and sigma-delta strategies for data conversion," *Electronics Communication Engineering Journal*, vol. 10, pp. 37–47, Feb 1998.

[32] P. Aziz, H. Sorensen, and J. vn der Spiegel, "An overview of sigma-delta converters," *Signal Processing Magazine, IEEE*, vol. 13, pp. 61–84, Jan 1996.

[33] J. Bacher, H. Köfler, and G. Maier, "The use of pitch factor in calculations of AC-machines with concentrated windings ," in *EPE 2005*, pp. 1–6, European Power Electronics and Drives Association, 2005.